Pergamon

Cement and Concrete Research 33 (2003) 499–507

CEMENT AND CONCRETE RESEARCH

Thickness effect on fracture energy of cementitious materials

Kai Duan[a,*], Xiao-Zhi Hu[a], Folker H. Wittmann[b,1]

[a]School of Mechanical Engineering, University of Western Australia, 35 Stirling Highway, Crawley, WA 6009, Australia
[b]Institute for Building Materials, Swiss Federal Institute of Technology, CH-8093, Zürich, Switzerland

Received 6 July 2001; accepted 13 September 2002

Abstract

This paper studies the thickness effect on the fracture energy of cementitious materials based on a local fracture energy concept. Similar to the specimen back boundary, the presence of two free surfaces in the thickness direction also influences the local fracture energy dissipation, leading to the boundary or thickness effect. A bilinear local fracture energy model originally developed to characterise the ligament or back boundary effect on the fracture energy is further developed to consider variations of the local fracture energy in the thickness direction. The proposed model is used to analyse available experimental data from the literature. The predictions from the model are in a good agreement with the experiments.

Keywords: Fracture energy; Size effect; Thickness effect; Ligament effect; Cementitious material

1. Introduction

Fracture properties of cementitious materials often exhibit strong size-dependence because of their coarse material structures and large fracture process zones (FPZ) created during crack growth. This has led to two major concerns for the application of fracture mechanics. Firstly, the fracture behaviour of laboratory-size specimens that can be easily tested in a laboratory cannot be simply extrapolated to large-scale practical concrete structures without a thorough understanding of the size effect. Secondly, direct measurements of fracture properties of large structure-like specimens are often beyond the capabilities of most laboratories. These concerns have been major driving forces behind the intensive research activities on the size effect.

Since Kaplan's work on the size effect in concrete fracture [1], many experimental observations on the size effect in fracture properties of concrete have be reported [2–6]. The size-effect law by Bažant [7,9] and Bažant and Pfeiffer [8] and the specific fracture energy G_F proposed by the RILEM [29–33] have further stimulated the interests in the size effect study. Extensive experimental and theoretical studies have been conducted to understand the size effect mechanisms and to obtain the size-independent fracture properties from experimental results measured from small laboratory-size specimens [10–25].

In general, size effect experiments of concrete reveal two common phenomena. Firstly, for geometrically similar specimens, concrete strength decreases with increasing specimen size although it does not follow exactly the Weibull's weakest link theory [7–9]. Secondly, both the specific fracture energy and fracture toughness increase with increasing specimen size and un-notched ligament length [1–6,21–25]. It should be mentioned here that the specimen thickness, as a size measurement, also influences the fracture behaviour of concrete. Unfortunately, comparing to the data on size/ligament effects, very limited experimental results on thickness effect are available in the literature. These limited experiments showed that the specific fracture energy increased with increasing specimen thickness and appeared to reach a plateau value when the specimen thickness increased to about four times of the maximum aggregate size [23–26]. Other reports showed that the thickness effect could not be detected if specimen thickness was much larger than the material maximum grain size [27,28].

A number of size effect models have been proposed to characterise the size effect on concrete fracture properties

* Corresponding author. Tel.: +61-8-9380-3124; fax: +61-8-9380-1024.
E-mail address: kaiduan@mech.uwa.edu.au (K. Duan).
[1] Present address: Qingdao Institute of Architecture and Engineering, Centre for Durability, Maintenance, and Repair, Qingdao, PR China.

0008-8846/02/$ – see front matter © 2002 Elsevier Science Ltd. All rights reserved.
PII: S0008-8846(02)00997-3

[7–19]. While these models have predominantly been focused on the effect of a characteristic size (e.g., width) or the un-notched ligament of specimens, there is hardly any theoretical model considering the limited experimental observations of the thickness effect on concrete fracture. Because of the very limited information on the thickness effect, the thickness of fracture mechanics specimens of concrete was set either constant (the same thickness effect, if any) or larger than four times of the maximum grain size to minimise the thickness effect [1–6,21–28]. It is difficult to justify whether four-times of grain-size can rule out any thickness effect without further experiments. That is more experiments and analytical work are necessary to gain a better understanding of the thickness effect mechanisms and to predict the fracture behaviour of concrete structures/specimens subjected to the thickness effect.

It has been shown recently through a boundary effect concept that the size effect on fracture properties can be related to the interactions between a crack, FPZ and specimen boundaries [13–20]. According to the boundary effect concept [17–19], the fracture energy dissipation remains constant at locations far away from a free boundary, but decreases sharply when a crack is approaching to a free boundary. Using a bilinear energy distribution function to approximate the fracture energy distribution, it has been shown that the common size effect is, in fact, due to the influence of a free specimen boundary [17–19]. In the present paper, the bilinear model is adopted to explain the thickness effect on concrete fracture. The major objectives of this current paper are to explain the size/thickness effect on concrete fracture through the boundary effect concept [17–19], and to model the thickness effect and compare with the available experimental results.

2. Influence of free surface on fracture energy

2.1. Concept of local fracture energy and ligament effect

The RILEM recommended specific fracture energy G_F is defined as the fracture energy necessary to create a unit crack area, and is commonly estimated from the applied load (P) and load-point displacement (δ) curve using the following equation [33],

$$G_F = \frac{1}{(W-a)B}\int P d\delta \tag{1}$$

where W is the specimen width, B is the thickness and a is the initial crack/notch length. According to Eq. (1), the total fracture energy $\int P d\delta$ is averaged over the entire fracture area $(W-a)B$, and the averaged fracture energy is G_F. As nearly all the fracture energy is consumed within the FPZ [29–31], the fracture energy G_F can be translated to the area under the cohesive stress-crack opening displacement ($\sigma_b - w$) curve according to the energy conservation principle, i.e.,

$$G_F = \int_0^{w_c} \sigma_b dw \tag{2}$$

where w_c is the critical crack opening displacement. The $\sigma_b - w$ curve is commonly accepted as a material property and, therefore, is independent of specimen geometry and size, and loading conditions. In other words, G_F from Eq. (2) is also a material constant. As a result, G_F defined in Eq. (1) should be independent of the specimen width W, initial crack length a and thickness B, as the RILEM recommendations originally assumed.

However, many experimental observations have clearly shown size/geometry and crack/ligament dependence of the specific fracture energy G_F defined in Eq. (1) (e.g., Refs. [1–6,17–26]). Besides many other studies and models on the size effect (e.g., Refs. [7–20]), the size effect on G_F has further been explained by a local fracture energy concept proposed by Hu and Wittmann [34,35]. Before proceeding to the details, it is helpful to clarify the fracture energy symbols used in order to avoid any confusion. In the following analysis and discussion, G_f will be used if the RILEM specific fracture energy is size dependent, and G_F will be used exclusively for the size-independent specific fracture energy. Therefore, G_F is the asymptotic value of G_f when a specimen size is very large.

To explain the local fracture energy concept [34,35], let us consider a specimen with a fixed thickness so that any thickness effect is not considered. As shown in Fig. 1, the FPZ or damage zone around a propagating crack in the specimen can be ideally divided into two regions, an inner softening zone (W_{sf}) and an outer microfracture zone (W_f) [34,35]. The inner softening zone contains interconnected fracture activities such as microcrack coalescing, zigzag cracking, crack branching and aggregate/grain interlocking,

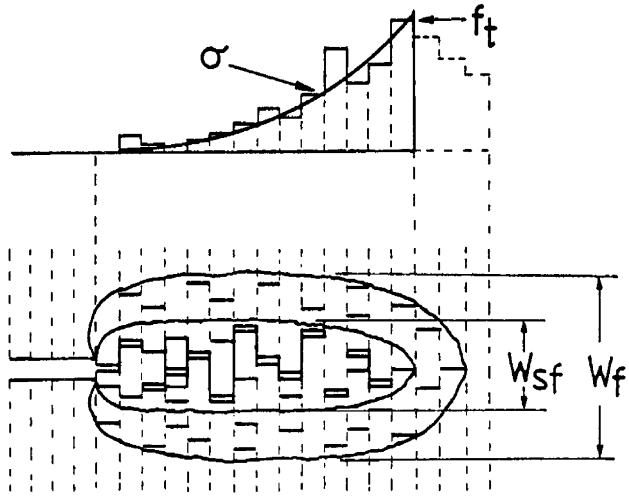

Fig. 1. The FPZ and discrete bridging stresses. The FPZ is divided into the inner softening zone and the outer microfracture zone. w_c is related to the width of the softening zone W_{sf} [34,35].

which are responsible for the concrete tensile softening behaviour. The outer microfracture zone consists mainly of isolated microcracks that are responsible for the nonlinearity in the tensile stress–strain relationship before tensile softening. That is the critical crack opening w_c is primarily determined by the fracture activities in the inner strain zone W_{sf}. Subdividing the FPZ into a number of thin tensile strips, the critical crack opening w_i for each thin strip or small tensile specimen should be proportional to its inner softening zone height. The specific fracture energy calculated using the critical local crack opening w_i and Eq. (2) is defined as the local fracture energy g_f, which should also be proportional to the inner softening zone height [34,35]. Let x denote the distance of a position along the un-notched ligament to the initial crack tip, the local fracture energy $g_f(x)$ can be related to the local critical crack opening $w_c(x)$ and FPZ height by [34,35]

$$\begin{aligned} W_{sf}(x) &\propto W_f(x) \\ w_c(x) &\propto W_{sf}(x) \\ g_f(x) &\propto w_c(x). \end{aligned} \tag{3}$$

Because the FPZ height does not remain constant over the entire un-notched ligament, and decreases rapidly when approaching a free boundary [36–40], the specific fracture energy defined in Eq. (1) is dependent on specimen size and geometry, and loading conditions. This size-dependent specific fracture energy G_f is in fact, an average of different local fracture energy $g_f(x)$ values over the entire un-notched ligament, i.e.,

$$G_f = \frac{1}{(W-a)} \int_0^{W-a} g_f(x)\mathrm{d}x. \tag{4}$$

Eqs. (3) and (4) do not include the thickness effect on the fracture energy. Under this condition, the FPZ and local fracture energy g_f can be considered in a two-dimensional system. For a more general case, the local fracture energy g_f will vary in both the ligament and thickness directions and, therefore, should be considered in a three-dimensional space.

Let us consider a specimen with width W, thickness B and initial crack length a (Fig. 2a). To define the local g_f that varies in both ligament and thickness directions, a Cartesian coordinate system with its origin at the middle of the initial crack front edge is attached to the specimen for convenience of the analysis. In this coordinate system, the g_f function contains two variables, x and y that represent the distances of a position in the ligament area to the back boundary and a thickness surface, and the specific fracture energy $G_f(a,B)$ can be related to the local fracture energy $g_f(x,y)$ by

$$G_f(a,B) = \frac{2}{B(W-a)} \int_0^{B/2} \int_0^{W-a} g_f(x,y)\mathrm{d}x\mathrm{d}y \tag{5}$$

where the energy symbol $G_f(a,B)$ is used to indicate that the specific fracture energy G_f is influenced by both the initial crack length a (or initial un-notched ligament $W-a$) and thickness B. Two dimensionless functions $q_W(x)$ and $q_B(y)$ need to be introduced into the g_f function to consider g_f variations in the ligament and thickness directions, i.e.,

$$g_f(x,y) = G_F \cdot q_W(x) \cdot q_B(y) \tag{6}$$

where G_F is a size-independent material constant. According to Eq. (3), $q_W(x)$ is proportional to the FPZ height distribution along the initial un-notched ligament and $q_B(y)$ is proportional to FPZ height distribution in the thickness direction. Substitute Eq. (6) into Eq. (5), $G_f(a,B)$ is obtained as

$$\begin{aligned} G_f(a,B) &= G_F \cdot Q_W(W-a) \cdot Q_B(B) \\ Q_W(W-a) &= \tfrac{1}{W-a} \int_0^{W-a} q_w(x)\mathrm{d}x \\ Q_B(B) &= \tfrac{2}{B} \int_0^{B/2} q_B(y)\mathrm{d}y. \end{aligned} \tag{7}$$

Again, G_F is a material constant. q_W and q_B and Q_W and Q_B are nondimensional parameters.

Using the assumptions in Eq. (3), the nondimensional functions $q_W(x)$ and $q_B(y)$ can be related to FPZ developed over the entire fracture process. A number of experimental observations and numerical analyses have been carried out to investigate the FPZ formation. These studies have shown that the FPZ height remains relatively consistent at the locations far away from a specimen back boundary, but diminishes rapidly when approaching the back boundary [36–40]. That is the formation of FPZ cannot be separated from the crack-tip stress field and the influence of a boundary on the stress field. The area enclosed by an isostress contour (proportional to the FPZ area) decreases rapidly when a crack is approaching to the back surface [30]. Computer simulations using nonlocal smeared-cracking finite element models show that the local fracture energy g_f varies along an un-notched ligament together with the FPZ height [40].

We have previously proposed a bilinear function to describe the g_f distribution due to the ligament effect, and shown that the predictions from the bilinear model are in good agreement with experimental observations [17,18]. The bilinear form of $q_W(x)$ is illustrated in Fig. 2b and c. Fig. 2b shows that the bilinear $q_W(x)$ function consists of two straight lines that intersect at a transition ligament a_l*. The parameter a_l* introduced by the present bilinear model is dependent on material properties, loading configuration and specimen geometry and size as it indicates the influence of these parameters on the FPZ formation. If a specimen has an initial un-notched ligament length $(W-a)$ longer than the

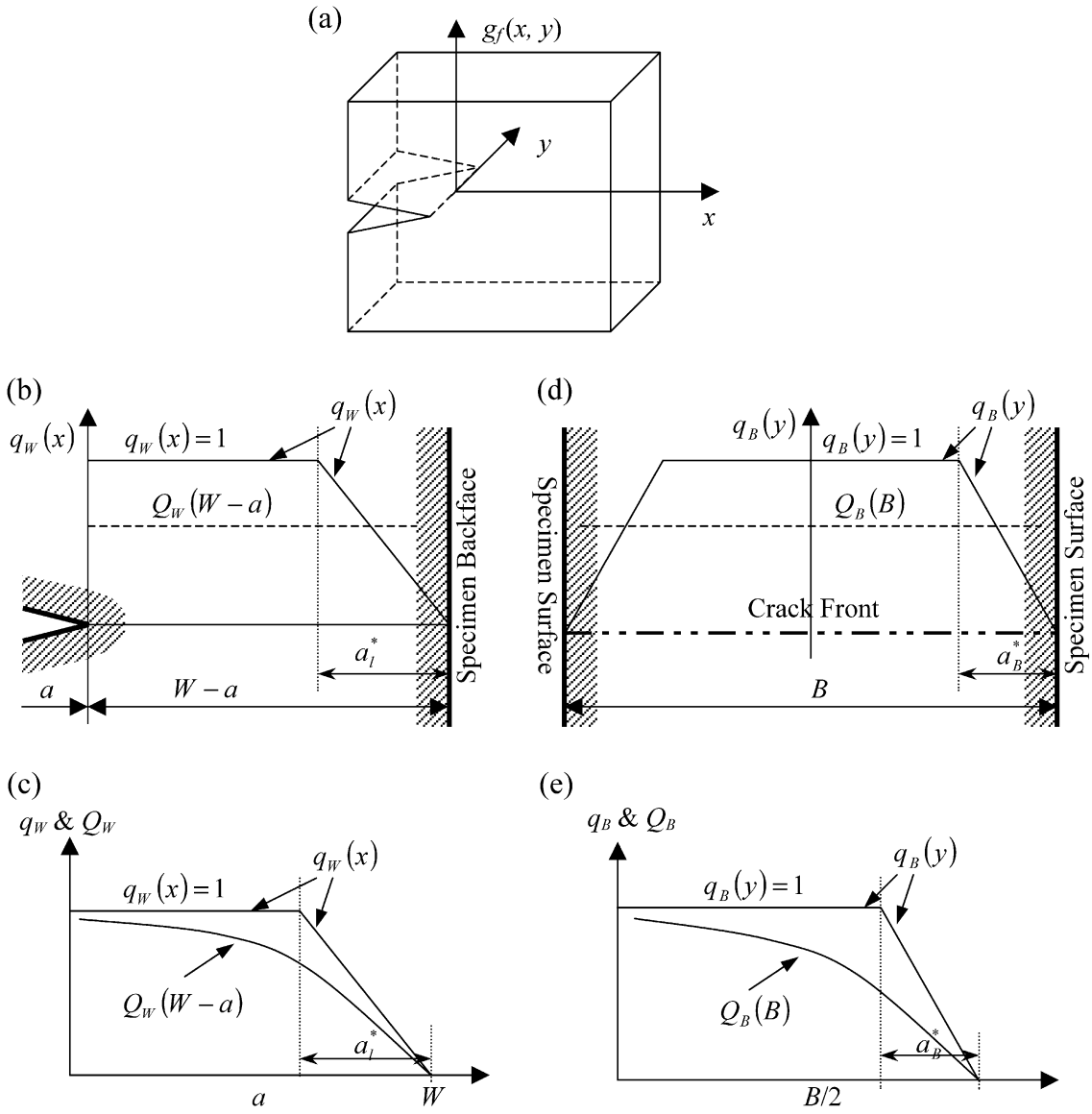

Fig. 2. The bilinear model of local fracture energy g_f: (a) Cartesian coordinate system for defining g_f, (b) the bilinear model of ligament effect, (c) the distribution of fracture energy (G_f and g_f) along the ligament, (d) the bilinear model of thickness effect, and (e) the distribution of fracture energy (G_f and g_f) in the thickness direction.

transition ligament a_1*, the dimensionless function $q_W(x)$ is written as [17,18]

$$q_W(x) = \begin{cases} 1 & x < W - a - a_1* \\ \frac{(W-a)-x}{a_l*} & x \geq W - a - a_1* \end{cases}. \quad (8)$$

If $W-a$ is smaller than the ligament transition length, the first function in the above equations disappears. The dashed horizontal line in Fig. 2b is $Q_W(W-a)$ as defined in Eq. (7), which is the average of the bilinear $q_W(x)$ function over the un-notched ligament $(W-a)$. The $Q_W(W-a)$ function has a value between 0 and 1 reflecting the effect of un-notched ligament length on the fracture energy. As shown in Fig. 2c, $Q_W(W-a)$ decreases with increasing crack length or decreasing un-notched ligament for a given specimen size of W. If a specimen has an un-notched ligament significantly longer than the transition ligament a_1*, $Q_W(W-a)$ is close to 1 and the fracture energy measured on the specimen will be independent of un-notched ligament size, i.e., $G_f \rightarrow G_F \cdot Q(B)$.

2.2. Thickness effect on fracture energy

To consider the thickness effect on the fracture energy G_f, it is necessary to examine how a free surface in the thickness direction influences the FPZ size and therefore, the g_f distribution in the thickness direction. Because a free surface in the thickness direction is also a free boundary, its influence on the FPZ height and g_f value is expected to be

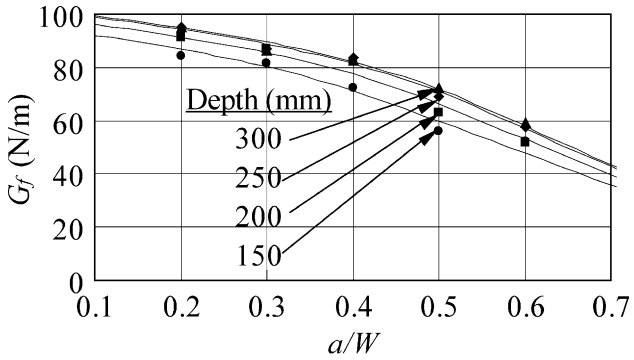

Fig. 3. The comparison of the predictions from Eq. (10) with the measured fracture energy data given in Refs. [5,6].

similar to that of a back specimen boundary. Therefore, the g_f distribution in the thickness direction should be similar to that along the ligament, i.e., the g_f remains constant at the locations far away from both free thickness surfaces, and diminishes rapidly when approaching a free thickness surface. Based on such a g_f distribution, crack propagation will start from specimen surface(s) and grows inwards because less energy is needed to propagate in this way. Such a crack growth pattern has been supported by a number of experimental observations [41–44].

From the above discussion, it is clear that the g_f distribution in the thickness direction can also be approximated by a bilinear function similar to the case of the ligament effect. Because of geometry symmetry, only half of the thickness needs to be considered. Within the half thickness, the dimensionless function $q_B(y)$ can be approximated by a bilinear function as shown in Fig. 2d and e. These two straight lines intersect at a_B* that is referred to as the transition thickness. Like a_l*, the a_B* is also dependent on material property, loading configuration and specimen geometry and size. For a specimen with a thickness larger than two times of a_B*, the bilinear function is written as

$$q_B(y) = \begin{cases} 1 & y \le \frac{B}{2} - a_B^* \\ \frac{\frac{B}{2}-y}{a_B^*} & y > \frac{B}{2} - a_B^* \end{cases}. \tag{9}$$

The first function will disappear for a thin specimen with thickness less than two times of a_B*. It should be mentioned here that all discussions on the function $q_W(x)$ in the previous section apply to the function $q_B(y)$.

Having formulated the local fracture energy distributions in both ligament and thickness directions, the ligament- and thickness-dependent specific fracture energy $G_f(a,B)$ can be easily obtained. Substitute Eqs. (8) and (9) into Eq. (7) and complete the integral calculations, the $G_f(a,B)$ can be written as

$$G_f(a,B) = G_F \cdot Q_W(W-a) \cdot Q_B(B)$$

$$Q_W(W-a) = \begin{cases} \frac{W-a}{2a_l^*} & \frac{W-a}{a_l^*} \le 1 \\ 1 - \frac{a_l^*}{2(W-a)} & \frac{W-a}{a_l^*} > 1 \end{cases} \tag{10}$$

$$Q_B(B) = \begin{cases} \frac{B}{4a_B^*} & \frac{B}{a_B^*} \le 2 \\ 1 - \frac{a_B^*}{B} & \frac{B}{a_B^*} > 2 \end{cases}.$$

As before, G_F is the size-independent fracture energy.

3. Analysis of experimental results

3.1. Ligament-dependent fracture energy

There are a number of experimental studies on the fracture energy G_f measured from the specimens with fixed size and thickness, but various notch lengths (e.g., Refs. [5,6,23,24,34,35]). The experimental data can be used to determine the function $Q_W(W-a)$ in Eq. (10) and, therefore, predict the ligament effect on the fracture energy G_f. In this paper, three-point bending tests by Nallathambi et al. [5,6] are used to explain the application of the present model to ligament effect on fracture energy.

Nallathambi et al. [5,6] tested the influence of various factors including specimen size, crack length, span, aggregate texture and size, and water/cement ratio on the fracture energy G_f and proposed an empirical equation to account for these factors. Their experiments clearly showed that the ratio of specimen depth W to span had a significant effect on the fracture energy G_f while other conditions are kept identical. The fracture energy data of 20-mm mix (maximum aggregate size) with identical depth-to-span ratio of 1/6 are used for the present study. The selected fracture energy data were measured on four groups of specimens with the same thickness of 80 mm and depths of 150, 200, 250 and 300 mm as plotted in Fig. 3. Apply Eq. (10) to the fracture energy values, the maximum fracture energy for thickness of 80 mm, $G_f(\infty,80)$ ($=G_F Q_B(80)$) and transition ligament length a_l* can be calculated, and the predicted parameters are listed in Table 1. Without results from thicker specimens, the $G_f(\infty,80)$ is taken as the size-independent specific fracture energy G_F since the thickness is four times of the maximum grain size [24,26]. The

Table 1
Estimated specific fracture energy $G_f(\infty,80)$ and ligament transition length a_l* from Refs. [5,6] for the beams with different depths

W (mm)	$G_f(\infty,80)$ (N/m)	a_l* (mm)
150	129.5	80.6
200	139.6	106.7
250	134.1	117.9
300	129.0	131.4

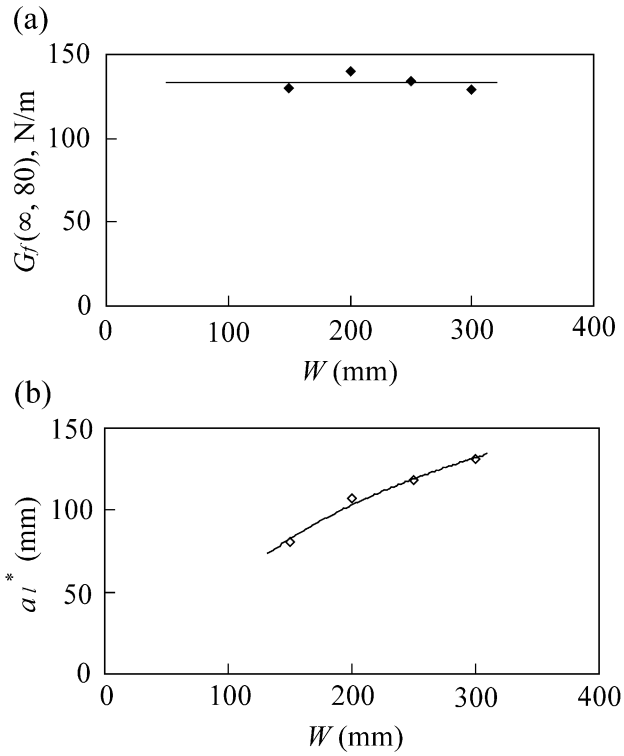

Fig. 4. The crack length-independent fracture energy $G_f(\infty,80)$ and the transition ligament a_l* as function of specimen depth W, predicted using Eq. (10).

predictions based on the parameters in Table 1 are shown in Fig. 3 to compare with those measured fracture energy G_f. It is seen that the predictions are in a good agreement with the experimental data. Some studies indicated that the minimum thickness required to avoid thickness effects may be much larger than four times of the maximum grain size. However, this does not influence the application of the ligament-effect formulae in Eq. (10) so long as the thickness is kept constant.

The results in Table 1 are plotted in Fig. 4 to show the relationship between specimen size and the parameters a_l* and $G_f(\infty,80)$. Fig. 4a shows that $G_f(\infty,80)$ from Eq. (10) is independent of the beam depth. Therefore, the fracture energy $G_f(\infty,80)$ for this concrete is estimated as 133.0 N/m by averaging those of the four $G_f(\infty,80)$ values in Table 1.

In contrast, the ligament transition length a_l* consistently increases with the specimen depth while the other conditions are kept unchanged (Fig. 4b). It appears a_l* would reach to a plateau with further increase in W. That is the boundary (or free surface) influence on the formation of FPZ will be saturated, and gradually, G_f will approach to $G_f(\infty,80)$. The variation in a_l* for small specimens is expected because it indicates the influence of a boundary, specimen size/geometry, and loading condition on the formation of FPZ.

3.2. Thickness effect on fracture energy

Thickness effect on the specific fracture energy G_f of various concrete materials was tested by Wittmann and colleagues [22–26]. The results from these studies showed a pronounced thickness effect for "thin" specimens. However, the thickness effect became undetectable when the specimen thickness increased to about four times of the maximum grain size partially due to the experimental scatters, and partially because only limited tests were performed.

In the present study, the fracture energy data of normal concrete with the maximum grain sizes of 8 and 32 mm, and an autoclaved aerated concrete (AAC) [22–26] was analysed by using the proposed model. These thickness effect experiments were performed using wedge-splitting specimens [22–26]. The square specimens measured by H vary from 100 to 400 mm, as shown in Table 2 together with thickness variation. W ($=H-15$ mm [22–26]) is the distance from the loading line to the specimen back surface. By applying Eq. (10) to these fracture energy data, the transition thickness a_B* and the maximum specific fracture energy $G_f(a,\infty)$ for a particular specimen (fixed W and a/W) can be calculated, and are listed in Table 2.

It can be seen that similar to the transition ligament a_l*, the transition thickness a_B* is also dependent on both the material microstructure and specimen size for normal con-

Table 2
The thickness effect parameters of the normal concrete and AAC from Refs. [22–26] estimated using Eq. (10)

Mater.	Max. aggregate (mm)	H (mm)	W (mm)	a/W	B (mm)	$G_f(a,\infty)$ (N/m)	a_B* (mm)	$G_f(a,B')$[a] (N/m)
Concrete[b]	32	100	85	0.50	50–200	150.50	3.70	146.15
		200	185	0.50		227.50	19.53	192.79
		400	385	0.50		275.00	13.51	245.98
Concrete[c]	32	200	185	0.62	10–200	170.05	13.79	151.73
Concrete[c]	8	200	185	0.62	10–80	125.52	3.50	111.79
AAC[d]		200	185	0.46–0.73	40–200	5.81	21.07	

[a] B' = four times the maximum aggregate size.
[b] Data from Ref. [25].
[c] Data from Ref. [24].
[d] Data from Ref. [23], G_F = 5.81 N/m and a_l* = 45.12 mm.

crete. For the AAC, the transition ligament a_1* and the size-independent fracture energy G_F are also given, as results from different a/W ratios are available.

The fracture energy values predicted using Eq. (10) and the parameters in Table 2 are plotted in Figs. 5 and 6 to compare with those measured. It can be seen that the fracture energy values calculated using this equation are in a good agreement with those experimental data. It is shown that the fracture energy $G_f(a,B)$ increases with the specimen thickness. Even when thickness B is four times of the maximum grain size, $G_f(a,B)$ is still 3–15% lower than the maximum fracture energy $G_f(a,\infty)$. This finding implies that one cannot rule out the thickness influence even if the specimen thickness is four times of the maximum grain size.

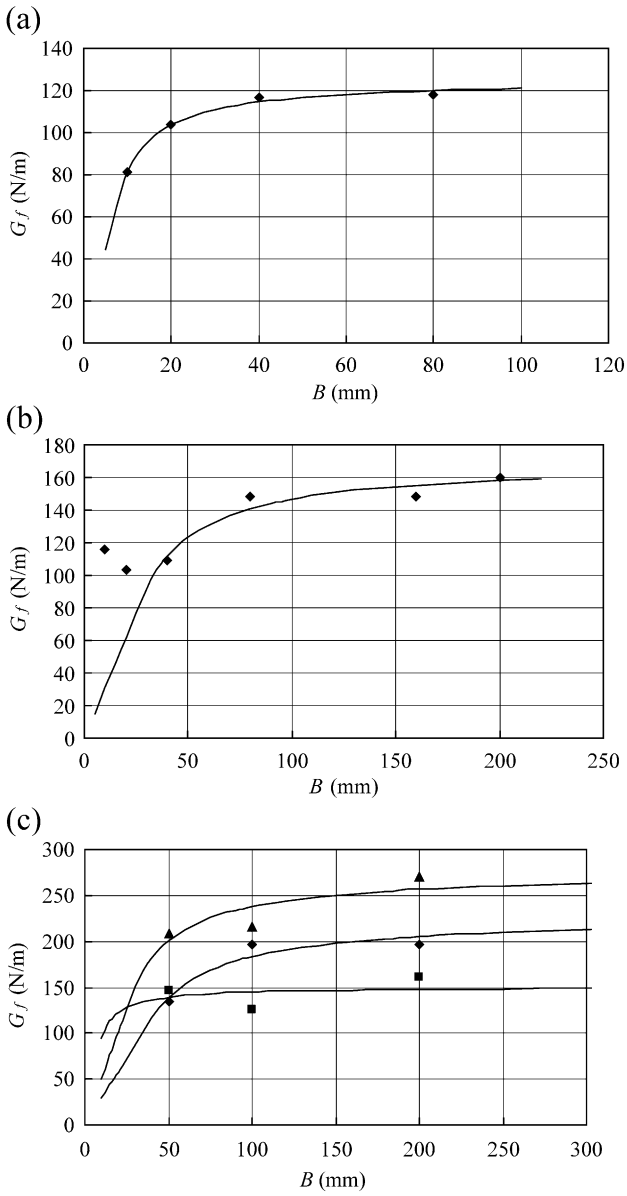

Fig. 5. The comparison of the predictions from Eq. (10) to the fracture energy measured on the specimens of normal concrete with the maximum grain size of (a) 8 mm from Ref. [24], (b) 32 mm from Ref. [24], and (c) 32 mm from Ref. [25].

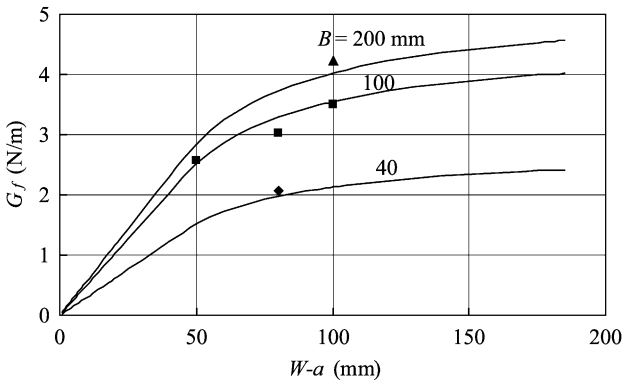

Fig. 6. The comparison of the predictions from Eq. (10) with the fracture energy measured on an AAC [23].

4. Discussion and conclusions

The present model on thickness effect is an extension of the bilinear model for the ligament effect on the fracture energy [17,18]. As a free surface in the thickness direction is also a free boundary, the thickness effect should be similar to the ligament effect. Therefore, previous discussions on the ligament effect also apply to the thickness effect.

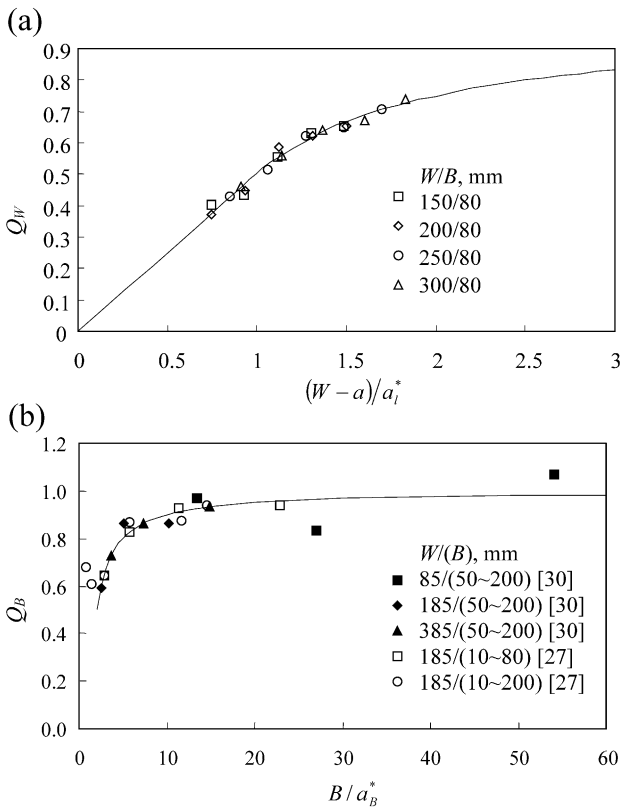

Fig. 7. The comparison of the theoretical curves of $Q_W(W-a)$ and $Q_B(B)$ with those measured data.

Based on the influence of a free boundary on the formation of FPZ, the two nondimensional local fracture energy functions, $q_W(x)$ and $q_B(y)$ in Eq. (6) have been approximated by two bilinear functions. Each bilinear function consists of a horizontal line with value of 1 and a declining straight line that reduces to zero at the free boundary. Because of the geometry symmetry, the bilinear function $q_B(y)$ represents the local g_f distribution in half of the thickness. The intersection of these two straight lines of $q_W(x)$ is defined as the transitional ligament a_l*, and the intersection of these two straight lines of $q_B(y)$ is referred to as the transition thickness a_B* as shown in Fig. 2. The validity of the proposed model is further indicated by Fig. 7 where the measured ligament and thickness effects on the fracture energy $Q_W(W-a)$ and $Q_B(B)$ are plotted to compare with the theoretical curves. These results show that suitable a_l* and a_B* can be defined for the bilinear fracture energy distributions although the bilinear assumption is very simple. As discussed in our previous work on the front face influence [13–16], both a_l* and a_B* are influenced by specimen size and geometry and loading conditions. However, stable a_l* and a_B* will be achieved for very large and thick specimens.

Eq. (10) further indicates the important roles of the two transitional lengths, a_l* and a_B*. These two parameters determine the extents of the effects of un-notched ligament and thickness on the measured specific fracture energy G_f. For example, the ligament and thickness effects on the specific fracture energy G_f measured on a specimen with an un-notched ligament larger than $10a_l$* and thickness larger than $20a_B$* are less than five percent. As a_l* and a_B* are dependent on both the material microstructures, loading conditions and specimen geometry/size, there is no simple relationship between these two parameters and the maximum grain size. However, for general discussions, we can conclude specimens with thickness less than $10a_B$* should be used to investigate the thickness effect for given specimen geometry and size and loading conditions. That explains why the thickness effect was observed by Wittmann and colleagues [23–26], but not by Mindess and Nadeau [27] and Tian et al. [28].

The thickness effect on the specific fracture energy G_f studied in this paper shows an opposite trend to that of metal fracture toughness, which increases with decreasing thickness [45]. These contrary trends result from different fracture mechanisms of these two types of materials. The size of a plastic zone in a metal specimen is increased when a crack tip is approaching to a free boundary because of the large scale yielding. The FPZ size measured in both length and height in a concrete specimen is decreased when a crack tip is approaching to a free boundary. Therefore, the plane stress condition due to the reduction in thickness promotes plastic deformation in metals, leading to high toughness. But the same thickness reduction in concrete limits the formation of FPZ and the intensity of frictional grain pull-out, leading to a reduced fracture energy.

Acknowledgements

The financial support from the Australian Research Council is acknowledged.

References

[1] M.F. Kaplan, Crack propagation and the fracture of concrete, ACI J. 58 (1961) 591–610.
[2] P.F. Walsh, Fracture of plain concrete, Indian Concr. J. 46 (1972).
[3] D.D. Higgins, J.E. Bailey, Fracture measurements on cement paste, J. Mater. Sci. 11 (1976) 1995–2003.
[4] S. Mindess, The effect of specimen size on the fracture energy of concrete, Cem. Concr. Res. 14 (1984) 431–436.
[5] P. Nallathambi, B.L. Karihaloo, B.S. Heaton, Effect of specimen and crack sizes, water/cement ratio and coarse aggregate texture upon fracture toughness of concrete, Mag. Concr. Res. 36 (129) (1984) 227–236.
[6] P. Nallathambi, B.L. Karihaloo, B.S. Heaton, Various size effects in fracture of concrete, Cem. Concr. Res. 15 (1985) 117–126.
[7] Z.P. Bažant, Size effect in blunt fracture: concrete, rock, metal, J. Eng. Mech. ASCE 110 (4) (1984) 518–535.
[8] Z.P. Bažant, P.A. Pfeiffer, Determination of fracture energy from size effect and brittleness number, ACI Mater. J. 84 (1987) 463–480.
[9] Z.P. Bažant, Size effect on strength: a review, Arch. Appl. Mech. 69 (1999) 703–725.
[10] A. Carpinteri, B. Chiaia, G. Ferro, Multifractal nature of material microstructure and size effects on nominal strength, in: G. Baker, B.L. Karihaloo (Eds.), Fracture of Brittle, Disordered Materials: Concrete, Rock and Ceramics, Proc. IUTAM Symposium, Brisbane, September 1993, E&FN Spon, London, 1995, pp. 21–34.
[11] A. Carpinteri, G. Ferro, S. Invernizzi, A truncated statistical model for analyzing the size-effect on tensile strength of concrete structures, in: F.H. Wittmann (Ed.), Fracture Mechanics of Concrete Structures (Proc. FRAMCOS-2), AEDIFICATIO Publishers, Freiburg, Germany, 1995, pp. 557–570.
[12] A. Carpinteri, B. Chiaia, Multifractal scaling law for the fracture energy variation of concrete structures, in: F.H. Wittmann (Ed.), Fracture Mechanics of Concrete Structures (Proc. FRAMCOS-2), AEDIFICATIO Publishers, Freiburg, Germany, 1995, pp. 581–596.
[13] X.Z. Hu, Size effects in toughness induced by crack close to free edge, in: H. Mihashi, K. Rokugo (Eds.), Fracture Mechanics of Concrete Structures (Proc. FRAMCOS-3), AEDIFICATIO Publishers, Freiburg, Germany, 1998, pp. 2011–2020.
[14] X.Z. Hu, An asymptotic approach to size effect on fracture toughness and energy, in: L. Ye, Y.W. Mai (Eds.), Proc. of Inter. Workshop on Fracture Mechanics and Advanced Engineering Materials, Dec. 8–10, Sydney, 1999, pp. 76–83.
[15] X.Z. Hu, F.H. Wittmann, Size effect on toughness induced by crack close to free surface, Eng. Fract. Mech. 65 (2000) 209–211.
[16] X.Z. Hu, An asymptotic approach to size effect on fracture toughness and fracture energy of composites, Eng. Fract. Mech. 69 (2002) 555–564.
[17] K. Duan, X.Z. Hu, F.H. Wittmann, Explanation of size effect in concrete fracture using non-uniform energy distribution, Mater. Struct. 35 (2002) 326–331.
[18] K. Duan, X.Z. Hu, F.H. Wittmann, Boundary effect on concrete fracture induced by non-constant fracture energy distribution, in: R. de Borst, J. Mazars, G. Pijaudier-Cabot, J.G.M. van Mier (Eds.), Fracture Mechanics of Concrete Structures, Proc. FRAMCOS-4, vol. 1, A.A. Balkema Publishers, Lisse, The Netherlands, 2001, pp. 49–55.
[19] K. Duan, X.Z. Hu, F.H. Wittmann, Size effect on fracture resistance and fracture energy of concrete, Mater. Struct. (in press).
[20] X.Z. Hu, Toughness measurements from crack close to free edge, Int. J. Fract. 86 (1997) L63–L68.

[21] F.H. Wittmann, H. Mihashi, N. Nomura, Size effect on fracture energy of concrete, Eng. Fract. Mech. 35 (1990) 107–115.
[22] B. Trunk, F.H. Wittmann, Experimental investigation into the size dependence of fracture mechanics parameters, in: H. Mihashi, K. Rokugo (Eds.), Fracture Mechanics of Concrete Structures (Proc. FRAMCOS-3), AEDIFICATIO Publishers, Freiburg, Germany, 1998, pp. 1937–1948.
[23] E. Brühwiler, J. Wang, F.H. Wittmann, Fracture of AAC as Influenced by Specimen Dimension and Moisture, J. Mater. Civil Eng. ASCE 3 (2) (1990) 136–146.
[24] X. Wittmann, H. Zhong, On some experiments to study the influence of size on strength and fracture energy of concrete (ETH Building Materials Reports No. 2, ETH Switzerland, 1994), AEDIFICATIO Publishers, 1996.
[25] B. Trunk, Einfluss der Bauteilgrösse auf die Bruchenergie von Beton (ETH Building Materials Reports No. 11, ETH Switzerland, 2000), AEDIFICATIO Publishers, 2000.
[26] F.H. Wittmann, Fracture process zone and fracture energy, in: Z.P. Bažant (Ed.), Fracture Mechanics of Concrete Structures (Proc. FRAMCOS-1), Elsevier, Amsterdam, 1992, pp. 391–403.
[27] S. Mindess, J.S. Nadeau, Effect of notch width on K_{IC} for mortar and concrete, Cem. Concr. Res. 6 (4) (1976) 529–534.
[28] M.-L. Tian, S.-M. Huang, E.-X. Liu, L.-Y. Wu, K.-Q. Long, Z.-S. Yang, Fracture toughness of concrete, in: F.H. Wittmann (Ed.), Fracture Toughness and Fracture Energy of Concrete, Proceedings of the International Conference on Fracture Mechanics of Concrete, Lausanne, Switzerland, October 1–3, 1985, Elsevier, Amsterdam, 1986, pp. 299–306.
[29] A. Hillerborg, M. Modeer, P.E. Petersson, Analysis of crack formation and crack growth in concrete by means of fracture mechanics and finite elements, Cem. Concr. Res. 6 (1976) 773–782.
[30] P.-E. Petersson, Crack Growth and Development of Fracture Zones in Plain Concrete and Similar Structures, Report TVBM-1006, Division of Building Materials Lund Institute of Technology, Sweden, 1981.
[31] A. Hillerborg, Analysis of one single crack, in: F.H. Wittmann (Ed.), Fracture Mechanics of Concrete, Elsvier, Amsterdam, 1983, pp. 223–249.
[32] A. Hillerborg, Results of three comparative test series for determining the fracture energy G_F of concrete, Mater. Struct. 18 (1985) 33–39.
[33] RILEM TC-50 FMC, Determination of the fracture energy of mortar and concrete by means of three-point bend tests on notched beams, Mater. Struct. 18 (1985) 287–290 (endorsed May 1993).
[34] X.Z. Hu, Fracture Process Zone and Strain Softening in Cementitious Materials (ETH Building Materials Reports No. 1, ETH Switzerland, 1990), AEDIFICATIO Publishers, Freiburg, Germany, 1995.
[35] X.Z. Hu, F.H. Wittmann, Fracture energy and fracture process zone, Mater. Struct. 25 (1992) 319–326.
[36] L. Cedolin, S. Dei Poli, I. Iori, Tensile behavior of concrete, J. Eng. Mech. Div. ASCE 113 (1987) 431–449.
[37] H. Mihashi, N. Nomura, Microcracking and tension-softening properties of concrete, Cem. Concr. Compos. 14 (1992) 91–103.
[38] K. Otsuka, H. Date, Fracture process zone in concrete tension specimen, Eng. Fract. Mech. 65 (2000) 111–131.
[39] Z.P. Bažant, F.-B. Lin, Nonlocal smeared cracking model for concrete fracture, J. Struct. Eng. ASCE 114 (11) (1988) 2493–2510.
[40] J. Bolander Jr., H. Hikosaka, Simulation of fracture in cement-based composites, Cem. Concr. Compos. 17 (1995) 135–145.
[41] A. Bascoul, F. Kharchi, J.C. Maso, Concerning the measurement of the fracture energy of a micro-concrete according to the crack growth in a three points bending test on notched beams, in: S.P. Shah, S.E. Swartz (Eds.), SEM/RILEM International Conference on Fracture of Concrete and Rock, Springer-Verlag, New York, 1989, pp. 396–408.
[42] S.E. Swartz, T.M.E. Refai, Influence of size effects on opening mode fracture parameters for precracked concrete beams in bending, in: S.P. Shah, S.E. Swartz (Eds.), SEM/RILEM International Conference on Fracture of Concrete and Rock, Springer-Verlag, New York, 1989, pp. 242–254.
[43] J.G.M. van Mier, Mode I fracture of concrete: discontinuous crack growth and crack interface grain bridging, Cem. Concr. Res. 21 (1991) 1–15.
[44] E.N. Landis, S.P. Shah, The influence of microcracking on the mechanical behavior of cement based materials, Adv. Cem. Basic Mater. 2 (1995) 105–118.
[45] D. Broek, Elementary Engineering Fracture Mechanics, 4th revised ed., Martinus Nijhoff Publishers, Dordrecht, 1986.